Arterial and portal venous liver perfusion using selective spin labelling MRI

Eur Radiol (2015) 25:1529–1540
DOI 10.1007/s00330-014-3524-z

HEPATOBILIARY-PANCREAS

Arterial and portal venous liver perfusion using selective spin labelling MRI

Hanke J. Schalkx · Esben T. Petersen · Nicky H. G. M. Peters · Wouter B. Veldhuis · Maarten S. van Leeuwen · Josien P. W. Pluim · Maurice A. A. J. van den Bosch · Marijn van Stralen

Received: 10 July 2014 / Revised: 10 October 2014 / Accepted: 18 November 2014 / Published online: 22 March 2015

Abstract
Purpose To investigate the feasibility of selective arterial and portal venous liver perfusion imaging with spin labelling (SL) MRI, allowing separate labelling of each blood supply.
Methods The portal venous perfusion was assessed with a pulsed EPISTAR technique and the arterial perfusion with a pseudo-continuous sequence. To explore precision and reproducibility, portal venous and arterial perfusion were separately quantified in 12 healthy volunteers pre- and postprandially (before and after meal intake). In a subgroup of 6 volunteers, the accuracy of the absolute portal perfusion and its relative postprandial change were compared with MRI flow measurements of the portal vein.
Results The portal venous perfusion significantly increased from 63±22 ml/100g/min preprandially to 132±42 ml/100g/min postprandially. The arterial perfusion was lower with 35±22 preprandially and 22±30 ml/100g/min postprandially. The pre- and postprandial portal perfusion using SL correlated well with flow-based perfusion (r^2=0.71). Moreover, postprandial perfusion change correlated well between SL- and flow-based quantification (r^2=0.77). The SL results are in range with literature values.
Conclusion Selective spin labelling MRI of the portal venous and arterial blood supply successfully quantified liver perfusion. This non-invasive technique provides specific arterial and portal venous perfusion imaging and could benefit clinical settings where contrast agents are contraindicated.
Key Points
- *Perfusion imaging of the liver by Spin Labelling MRI is feasible*
- *Selective Spin Labelling MRI assessed portal venous and arterial liver perfusion separately*
- *Spin Labelling based portal venous liver perfusion showed significant postprandial increase*
- *Spin Labelling based portal perfusion correlated well with phase-contrast based portal perfusion*
- *This non-invasive technique could benefit settings where contrast agents are contraindicated*

Keywords Liver · Magnetic resonance imaging · Perfusion imaging · Arterial Spin Labelling

Abbreviations

PVSL	portal venous spin labelling
ASL	arterial spin labelling
SL	spin labelling
DCE-MRI	dynamic contrast-enhanced magnetic resonance imaging
BMI	body mass index
SNR	signal-to-noise ratio
SE-EPI	spin-echo echo-planar imaging
TI	inversion time
VOI	volume-of-interest
TR	repetition time
PLD	post labelling delay

H. J. Schalkx (✉) · E. T. Petersen · W. B. Veldhuis · M. S. van Leeuwen · M. A. A. J. van den Bosch
Department of Radiology, University Medical Center Utrecht, HP E.01.132, Postbus 85500, 3508 GA Utrecht, The Netherlands
e-mail: h.schalkx@gmail.com

N. H. G. M. Peters
Department of Radiology, Atrium Medical Center Parkstad, Heerlen, The Netherlands

J. P. W. Pluim · M. van Stralen
Image Sciences Institute, University Medical Center Utrecht, Utrecht, The Netherlands

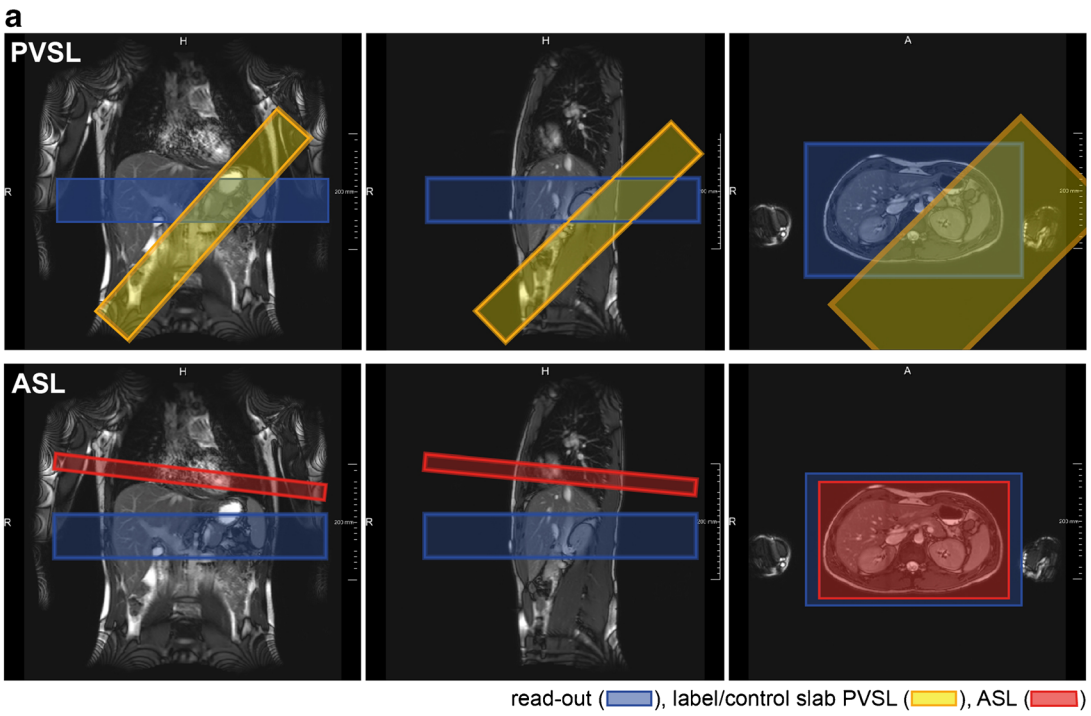
a
PVSL
ASL
read-out (), label/control slab PVSL (), ASL ()

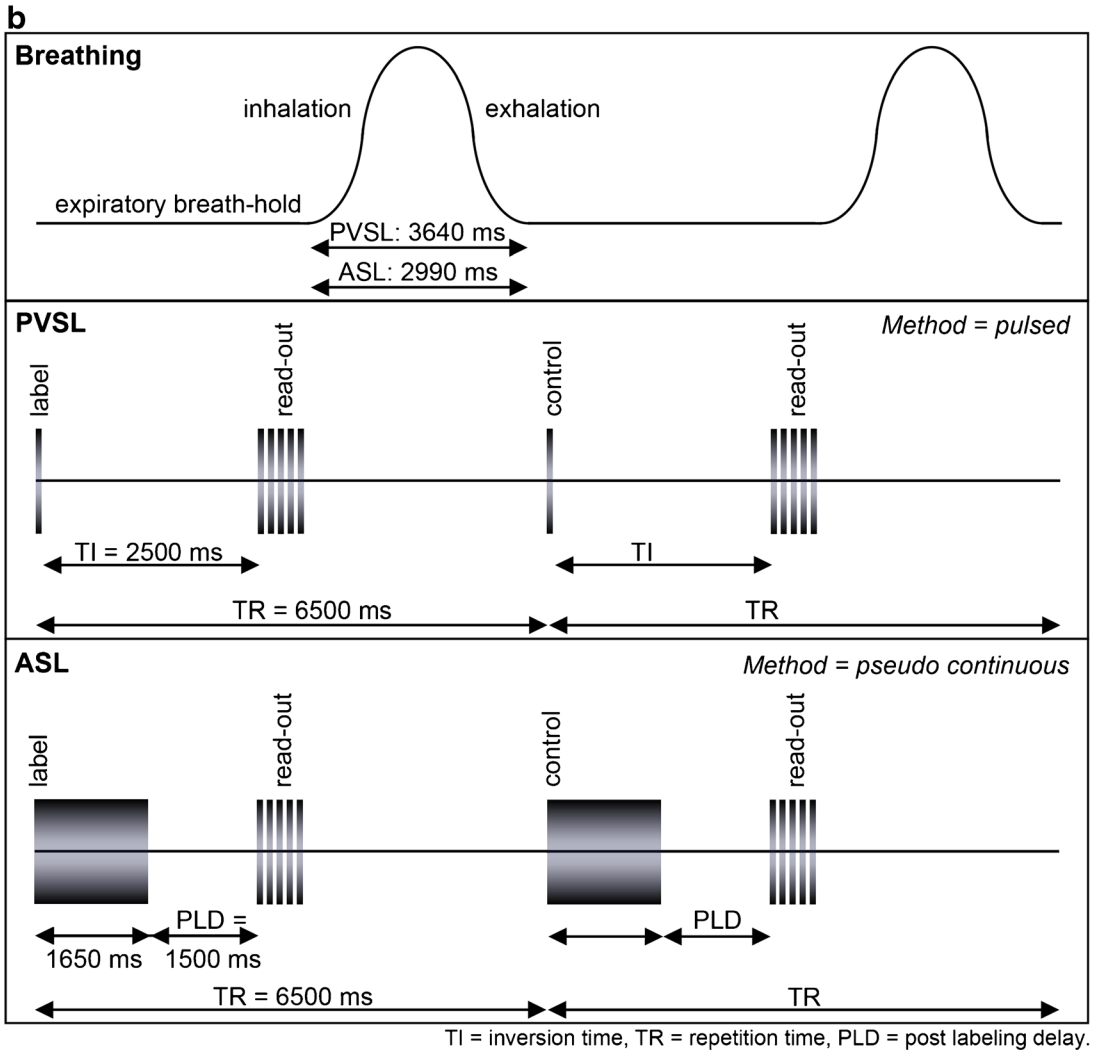
b
Breathing
inhalation
exhalation
expiratory breath-hold
PVSL: 3640 ms
ASL: 2990 ms
PVSL
Method = pulsed
label
read-out
control
read-out
TI = 2500 ms
TI
TR = 6500 ms
TR
ASL
Method = pseudo continuous
label
read-out
control
read-out
PLD = 1650 ms
1500 ms
PLD
TR = 6500 ms
TR
TI = inversion time, TR = repetition time, PLD = post labeling delay.

◀ **Fig. 1** Geometry and overview of the spin labelling sequences. **a** Geometry of the PVSL and ASL sequences: a transverse read-out (blue) centered around entry of the portal vein into the liver; an oblique label/control slab caudal of the liver for PVSL, labelling the portal vein and its feeding vessels; an oblique label/control slab transverse just above the diaphragm for ASL (red), labelling the arterial blood in the descending aorta. **b** An overview of pulsed PVSL and pseudo-continuous ASL protocols with the breathing signal. Scan parameters: TR of 6500 ms; TI of 2500 ms for PVSL; labelling duration and post-labelling delay of 1650 ms and 1500 ms, respectively, for ASL. Subjects were instructed to inhale and exhale after completion of each read-out and keep the expiratory breath-hold until the end of the corresponding read-out. Label/control excitations, labelling delay, and read-out took place during the breath-hold.

Introduction

Magnetic resonance imaging (MRI) of the liver plays a major role in the diagnosis and treatment monitoring of liver disease, where enhancement characteristics are evaluated after administration of a contrast agent [1]. Quantification of arterial and portal venous perfusion has aroused interest for characterization of perfusion patterns in focal and diffuse liver disease [1, 2].

Spin labelling MRI (SL-MRI) is a perfusion imaging technique using labelled protons in blood as an endogenous contrast for noninvasive quantification of blood flow [3]. Subtraction of images acquired in a labelling experiment from those in a control experiment allows estimation of the tissue perfusion. SL-MRI was initially introduced for brain perfusion imaging [4, 5]. Its application has been extended to organs other than the brain and oncological imaging. In abdominal organs, SL-MRI is almost exclusively performed in the kidneys [6–9]. Abdominal SL-MRI is especially challenged by possible misalignment between the control and label images. Furthermore, hepatic SL-MRI is challenged by the relatively low blood flow compared to the brain and its dual inflow.

However, SL-MRI has advantages of interest for liver imaging. Since SL-MRI is non-invasive, drug-related risks of exogenous contrasts are of no concern. In addition, SL-MRI allows for repeated imaging in the same session. This technique could therefore be helpful when administration of contrast agents is contraindicated or impractical, for example during minimally invasive treatments of focal liver lesions. During and after ablation treatments, MRI is increasingly used for assessment of the viable and non-perfused tissue and repeated contrast administration is thereby impossible. Regarding the dual inflow, the arterial and portal venous inflow could be selectively labelled and therefore be separately imaged and quantified.

Very few studies have described SL-MRI of the liver in humans, with promising results [10–13]. Only the study by Katada et al. [12] was published in a peer-reviewed journal. Katada et al. [12] examined selectively portal perfusion (5 healthy subjects) and compared the results with computed tomography (CT) portography in the same patients. Only Gach et al. [10] have studied selective arterial and portal venous perfusion, but in just a single healthy subject. In conclusion, selective arterial and portal SL-MRI perfusion imaging has been sparsely explored.

The aim of this study was to assess the feasibility of liver perfusion imaging with selective SL-MRI in healthy volunteers to separately quantify arterial and portal venous perfusion. Additionally, to explore the precision and reproducibility of the selective SL-MRI technique, two different perfusion conditions were evoked by scanning pre- and postprandially (before and after eating). Finally, to probe the portal SL-MRI accuracy, MRI flow measurements in the portal vein were performed in a subgroup.

Materials & methods

Study concept

For this feasibility study, the portal venous and arterial perfusion were assessed by pulsed portal venous spin labelling (PVSL) and pseudo-continuous arterial spin labelling (ASL) techniques, respectively, in healthy volunteers. For evaluation of the SL-MRI technique, the arterial and portal venous perfusion were imaged pre- and postprandially. By scanning every individual before and after ingestion of a high-calorie solid and high-sugar liquid meal, two different perfusion conditions were evoked and postprandial perfusion changes were evaluated. A postprandial increase in the portal blood flow is expected and primarily related to meal-induced splanchnic vasodilation and subsequent flow increase in the superior mesenteric vein [14]. Postprandial scans were planned around the time of expected portal venous peak flow. In a subgroup (N=6) the perfusion values were quantitatively compared to mean perfusion obtained via MRI flow measurements in the portal vein.

Subjects

Twelve healthy volunteers (seven male, five female) with no history of liver disease were enrolled in this study. Subjects were imaged in supine position on a 1.5 T MR Ingenia system (Philips Healthcare, Best, The Netherlands) equipped with an anterior and posterior 28-channel coil. Mean age and body mass index (BMI) were 28±4 years and 23±2 kg/m^2, respectively. Written informed consent was obtained from all subjects.

Experiments

For each subject, the imaging protocol was as follows: preprandial images were obtained in an imaging session of

30 minutes; then, the meal was ingested during a 30-minute break; then a 30-minute postprandial imaging session followed. All subjects were instructed to fast for at least two hours before the start of the measurements.

Pre- and postprandial imaging sessions included respiratory-triggered transverse T1-weighted acquisitions, a pulsed portal venous spin labelling (PVSL) sequence, and a pseudo-continuous arterial spin labelling (ASL) sequence. In the latter 6 of the 12 subjects, a phase-contrast flow sequence of the portal vein was added pre- and postprandially. The flow measurements (Q-flow software, Philips Healthcare, Best, The Netherlands) in the portal vein served as a comparison for portal venous perfusion by scaling the measured bulk flow with the liver volume and density.

MRI technique

The PVSL sequence was performed as a pulsed spin labelling experiment (EPISTAR [15]) benefiting from a high labelling efficiency [16] and adaptable bolus width [17]. An oblique labelling slab of 150 mm was used, positioned caudal of the liver covering the portal vein and its feeding vessels (see Fig. 1a). After empirical optimization (see Fig. 2) of the inversion time, a TI of 2500 ms (similar to [12]) was used in the PVSL experiments to achieve optimal signal-to-noise ratios (SNRs). Image read-out was a multislice 2D spin-echo echo-planar imaging (SE-EPI) sequence with SPIR fat suppression (TE=18.4 ms, EPI factor 53, manual TR=6500 ms, flip angle 90°, matrix 128×128, voxel size 2.9×2.9 mm, slice thickness 8.0 mm, slice gap 0.8 mm, parallel imaging factor 2, slices acquired in ascending order). The transversal read-out slice-stack was centred on the insertion level of the portal vein into the liver.

The ASL sequence was performed as a pseudo-continuous labelling experiment [18]. A pseudo-continuous labelling strategy was chosen, with consequently a thin labelling slab, to avoid re-tagging of spins after incomplete relaxation in the lungs and the heart which would occur in a pulsed labelling strategy such as the EPISTAR technique. A nearly transverse labelling slab of 10 mm was placed cranial to the diaphragm, labelling the arterial blood in the descending aorta (see Fig. 1a).

Labelling duration and delay were based on its parallels to the brain with comparable arterial blood flow velocity and distance from labelling slab to organ. After empirical optimization to reach a high SNR, these were set to 1650 ms and 1500 ms, respectively. Image read-out was similar to the PVSL experiment, although employing a gradient echo EPI instead, since our system unfortunately did not allow SE-EPI in combination with pseudo-continuous labelling (TE=18.4 ms, EPI factor 53, manual TR=6500 ms, flip angle 90°, parallel imaging factor of 2). The read-out was performed with the same geometry as the PVSL read-out.

All spin labelled sequences were performed with 20 label-control pairs and took 4 min 20 sec each. The geometry of the spin labelling experiments is illustrated in Fig. 1a, with an

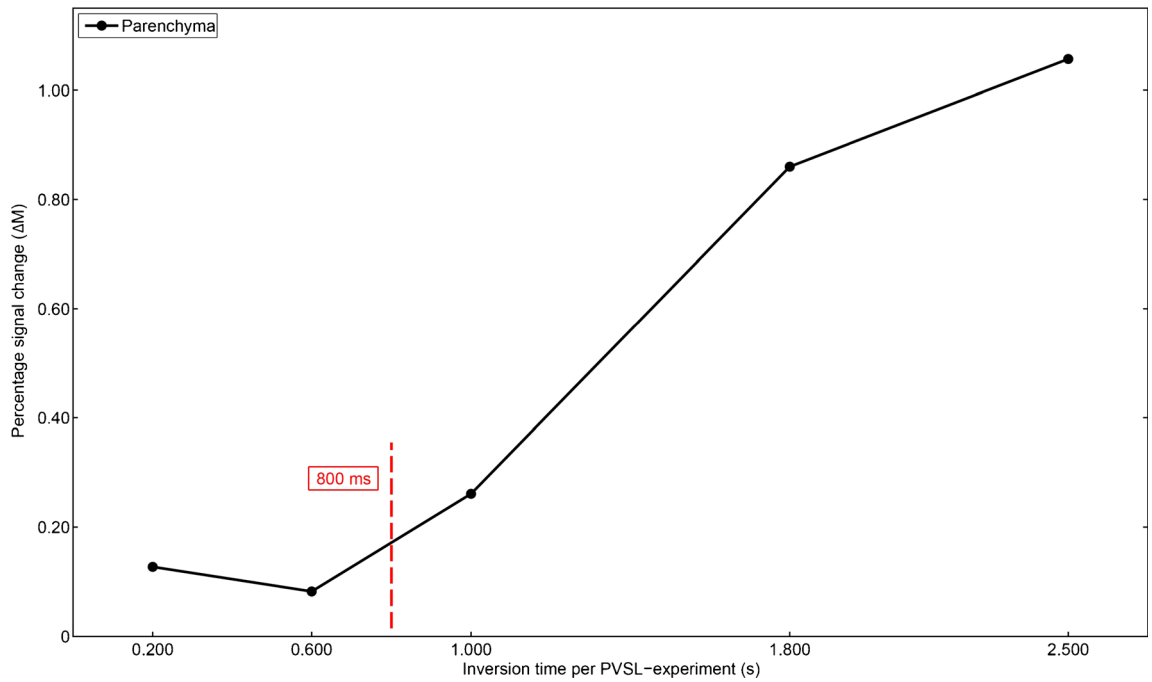

Fig. 2 Initial transit time. Multiple PVSL-experiments were performed in one healthy volunteer with varying inversion times (TI) (200, 600, 1000, 1800, and 2500 ms). The percentage signal change changed significantly between a TI of 600 and 1000 ms, with an assumed bolus arrival time of 800 ms as a consequence. A high perfusion signal change at a TI of 2500 ms supports use of this value for the PVSL-experiments

Table 1 Parameters of spin labelling sequences

PVSL	
Method	pulsed, EPISTAR
Readout	SE-EPI, 9 transverse slices, 8 mm, 0.8 mm spacing
Label	150 mm, oblique caudal of liver
TR	6500 ms, fixed
TI	2500 ms
ASL	
Method	Pseudo-continuous
Readout	GRE-EPI, 9 transverse slices, 8 mm, 0.8 mm spacing
Label	transverse above diaphragm
TR	6500 ms, fixed
Labelling time	1650 ms
PLD	1500 ms

PVSL=portal venous spin labelling, ASL=arterial spin labelling, SE=spin echo, EPI=echo planar imaging, TR=repetition time, TI=inversion time, GRE=gradient echo, PLD=post-labelling delay

overview of the PVSL and ASL protocol in Fig. 1b. An overview of the most important imaging parameters of the PVSL and ASL sequences is given in Table 1.

The flow measurements in the portal vein were performed using a single-slice, spoiled gradient echo phase contrast sequence during an expiratory breath-hold (TR/TE=6.3/4.1 ms, flip angle 12°, 4 averages, velocity encoding=50 cm/s). The 8-mm slice was placed perpendicular to the portal vein, close to the insertion of the portal vein into the liver.

Breathing synchronization

An overview of the timing of the PVSL and ASL sequence with respect to the breathing cycle is shown in Fig. 1b. As spin labelling acquisitions are sensitive to motion between the control and labelling experiments, careful breathing instructions were provided to image in expiratory state. Subjects were instructed to inhale and exhale in one go after completion of each read-out, which was easily recognised as an acoustic trigger. They were instructed to stay in expiratory breath-hold shortly until the next read-out was finished. During the breath-hold there was sufficient time for label or control excitations, labelling delay, and read-out. Since the repetition time (TR) was set to 6500 ms, there was 3640 ms for PVSL and 2990 ms for ASL reserved in each repetition for comfortable inhalation and exhalation.

Image analysis

Quantitative arterial and portal perfusion was derived from the spin labelling acquisitions. Label images were subtracted from their corresponding control images. The mean of subtractions was computed after manual exclusion of a few pairs with major artefacts caused by differences in breathing levels.

Portal venous perfusion was calculated voxel-wise from the PVSL acquisitions using the standard model as described by Buxton et al. (Eqn. 3, [19]). The arterial perfusion was calculated similar to the ASL experiments using Eqn. 5 for continuous labelling from [19]. See Table 2 for the quantification models and parameters.

The T_1-weighted images were manually segmented to include the entire liver, excluding the inferior caval vein, to define the volume-of-interests (VOI) for the perfusion measurements. As we targeted quantification of the parenchymal perfusion, we excluded large vasculature from the analysis.

Table 2 Quantification models and parameters for image analysis

Quantification models		
PVSL	$\Delta M(t) = 2M_{0B} f (t-\Delta t) \alpha e^{-t/T_{1B}} q_p(t)$	See Eqn. 3 in [19]
ASL	$\Delta M(t) = 2M_{0B} f T_1' \alpha e^{-\Delta t/T_{1B}} e^{-(t-\tau-\Delta t)/T_1'} \left(1-e^{-\tau/T_1'}\right)$ with $\frac{1}{T_1'} = \frac{1}{T_1} + \frac{f}{\lambda}$	See Eqn. 5 in [19]
Parameters		**Value**
$\Delta M(t)$	the signal difference after an inversion time t	
M_{0B}	Equilibrium magnetization of blood, estimated from average control image	
α	labelling efficiency, estimated to be 0.90 for PVSL and 0.85 for ASL	0.90 for PVSL, 0.85 for ASL
T_{1B}	T_1 of blood	1.58 s [34]
Δt	initial transit time	800 ms for PVSL, 1 s for ASL
	T1 of liver	0.586 s [35]
	Liver density	1060 kg/m^3 [36]
λ	Tissue-blood ratio	0.95 [31]

PVSL=portal venous spin labelling, ASL=arterial spin labelling

For comparison, portal venous flow velocity values were derived from the phase-contrast based quantitative flow measurements of the portal vein. Mean flow was measured by manually placing an elliptical region-of-interest (ROI) in the portal vein. The flow-based perfusion was estimated by $\frac{mean\ portal\ velocity * cross\ sectional\ area}{liver_{volume} * liver_{density}}$.

The bolus arrival time for PVSL was estimated with additional PVSL experiments in one volunteer postprandially with varying inversion times (200, 600, 1000, 1800, and 2500 ms). As a significant signal change was reached between 600 and 1000 ms, an initial transit time of 800 ms was used for the portal venous perfusion analysis (Fig. 2). For ASL Δt was set to one second, based on the longer transit time from labeling localization in the descending aorta into the liver.

All post-processing was done using in-house developed software based on the MeVisLab medical image processing and visualization environment (version 2.5, MeVis Medical Solutions, Bremen, Germany).

Statistical analysis

Assuming normality of hepatic perfusion rates [20], the paired samples Student's t-test was applied to assess differences in pre- and postprandial quantitative perfusion. A p-value of ≤ 0.05 was considered significant. Bland-Altman plots were constructed to provide information about the distribution of agreement between flow-based and SL-based perfusion and perfusion change. Statistical analyses were performed using SPSS software (version 20 for Windows, IBM statistics, Chicago, IL, USA).

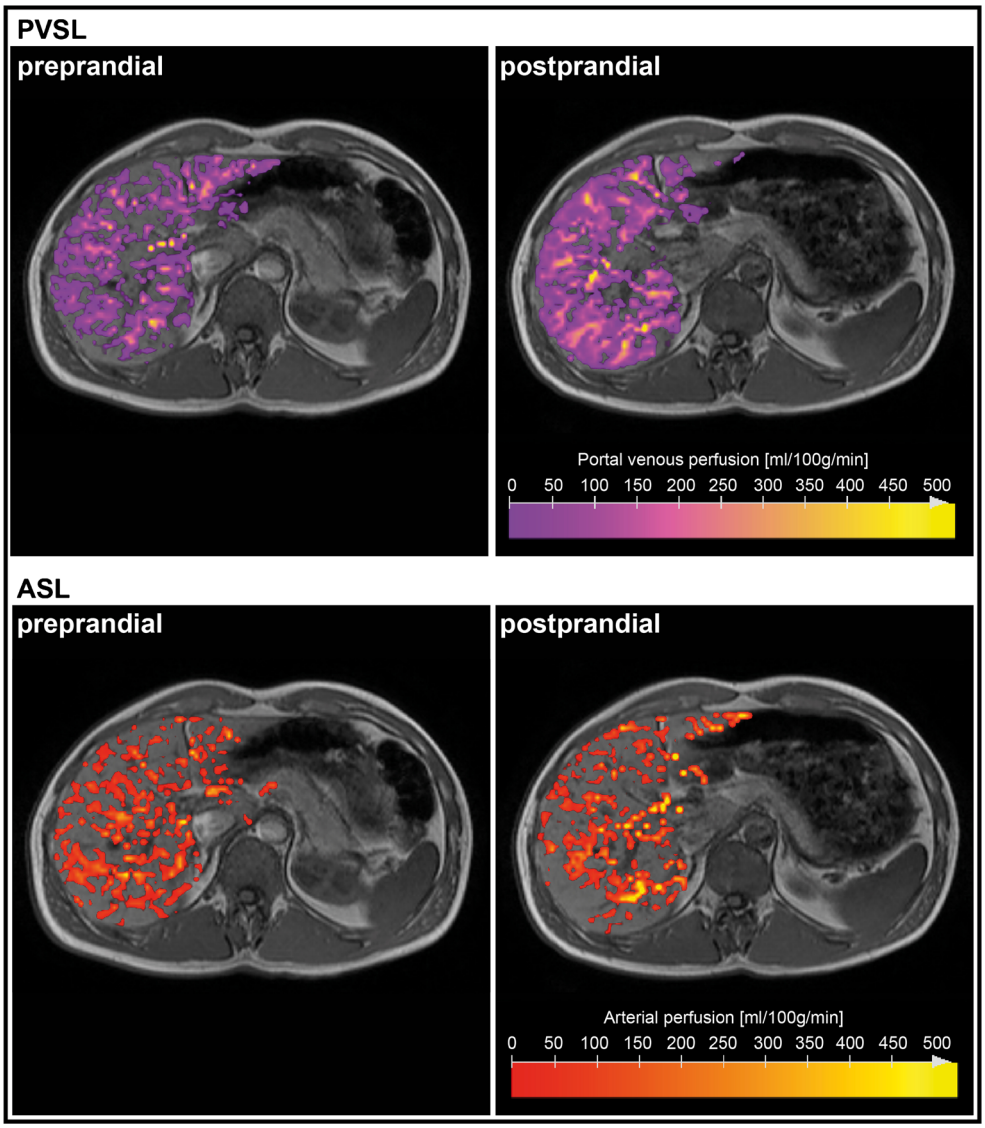

Fig. 3 Typical example of PVSL- and ASL-based perfusion. Portal venous (top row) and arterial perfusion (bottom row) with our spin labelling MRI experiments pre- (left) and postprandially (right)

Results

Experiments

All PVSL, ASL and Q-flow experiments were successfully performed. A typical example of the PVSL and ASL results is shown in Fig. 3. Breathing instructions were successfully followed by all subjects. On average, one (maximum of five) label-control pair per spin labelling scan were removed after visual examination due to breathing-related motion artefacts and EPI distortions, corresponding with an acceptance rate of 95 % (46 of the total 960 pairs were rejected).

Portal venous perfusion

Postprandial PVSL imaging was 45±3 min after the start of meal ingestion, with a minimum of 41 and a maximum of 52 min. The relative signal change $\Delta M(t)$ was 0.99±0.35 % preprandially and 2.07±0.66 % postprandially. The corresponding preprandial perfusion was 63±23 ml/100g/min and significantly increased to 132±42 ml/100g/min in the postprandial session ($p<0.001$). See Fig. 4a.

Portal perfusion was estimated using both PVSL and Q-flow measurements in the subgroup of six subjects. See Fig. 4b. The pre- and postprandial portal perfusion differed significantly for both PVSL- ($p=0.018$) and flow-based measurements ($p=0.011$). The PVSL perfusion values of 55±22 preprandially and 133±42 ml/100g/min postprandially correlated well ($r^2=0.70$) with the flow-based perfusions of 57±12 and 124±32 ml/100g/min, respectively, for the subgroup (Fig. 5a). The Bland-Altman plot (Fig. 5b) showed a mean difference between the two techniques of 3.1 ml/100g/min with 95 % limits of agreement (LOA) of [-56, 62]. Moreover, the postprandial perfusion change correlated well between PVSL- and flow-based quantification ($r^2=0.77$, Fig. 5c). The Bland-Altman plot of the PVSL- versus flow-based portal perfusion change (Fig. 5d) showed a mean difference of 11 ml/100g/min with 95 % LOA of [-44, 65]. An overview of the liver perfusion results is shown in Table 3.

Arterial perfusion

Postprandial ASL imaging was 39±3 min after the start of meal ingestion, with a minimum of 36 and a maximum of 47 min. Visual evaluation of the ASL images showed clear perfusion of the renal cortex, confirming successful labelling of arterial blood. In agreement with the literature [21], the relative signal changes of 0.12±0.08 % and 0.08±0.11 % pre- and postprandially (N=12) were lower than the portal venous counterparts. The same holds for the corresponding arterial perfusion values, with no significant difference ($p=0.27$) between the preprandial and postprandial values of 35±22 and 22±30 ml/100g/min, respectively. An overview of the perfusion results is presented in Table 3.

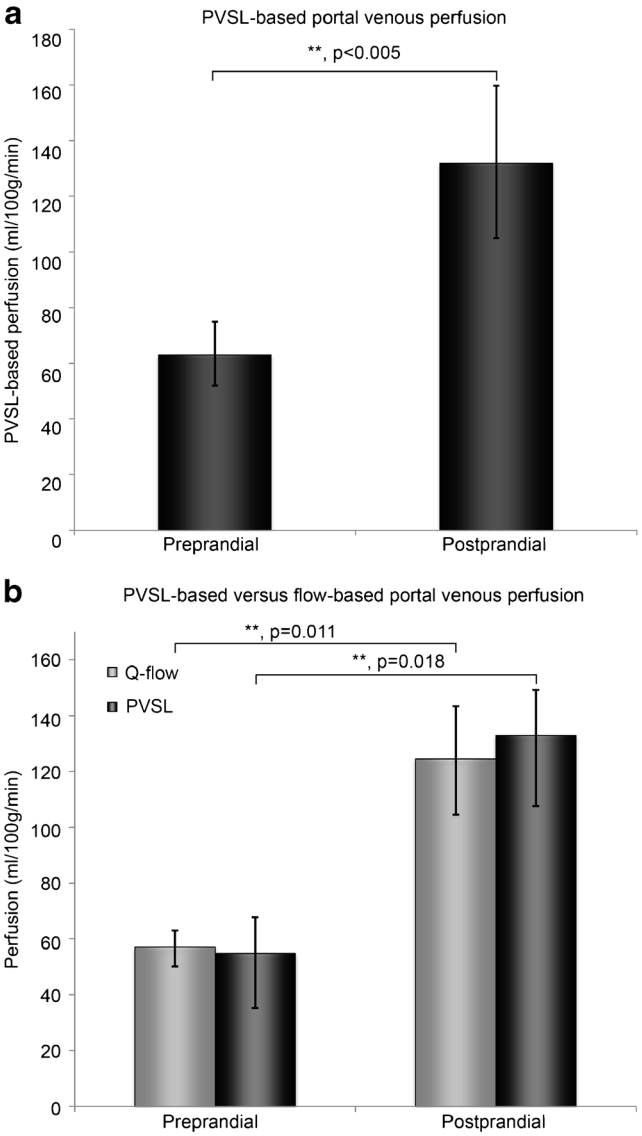

Fig. 4 Pre- and postprandial portal venous perfusion. **a** Pre- and postprandial portal venous perfusion based on PVSL-measurements. The perfusion rates of mean and standard deviation of 63±23 and 132±42 ml/100g/min, respectively, differed significantly ($p<0.001$). **b** Flow-based portal venous perfusion was 57±12 and 124±32 ml/100g/min, pre- and postprandially (N=6). PVSL-based portal venous perfusion was 55±22 pre- versus 133±49 ml/100g/min postprandially in this subgroup (N=6). The whiskers denote the 25th- and 75th- percentile values of the distributions

Discussion

This study demonstrates that selective spin labelling MRI of the portal venous and arterial blood supply can be used to non-invasively quantify arterial and portal liver perfusion in healthy volunteers.

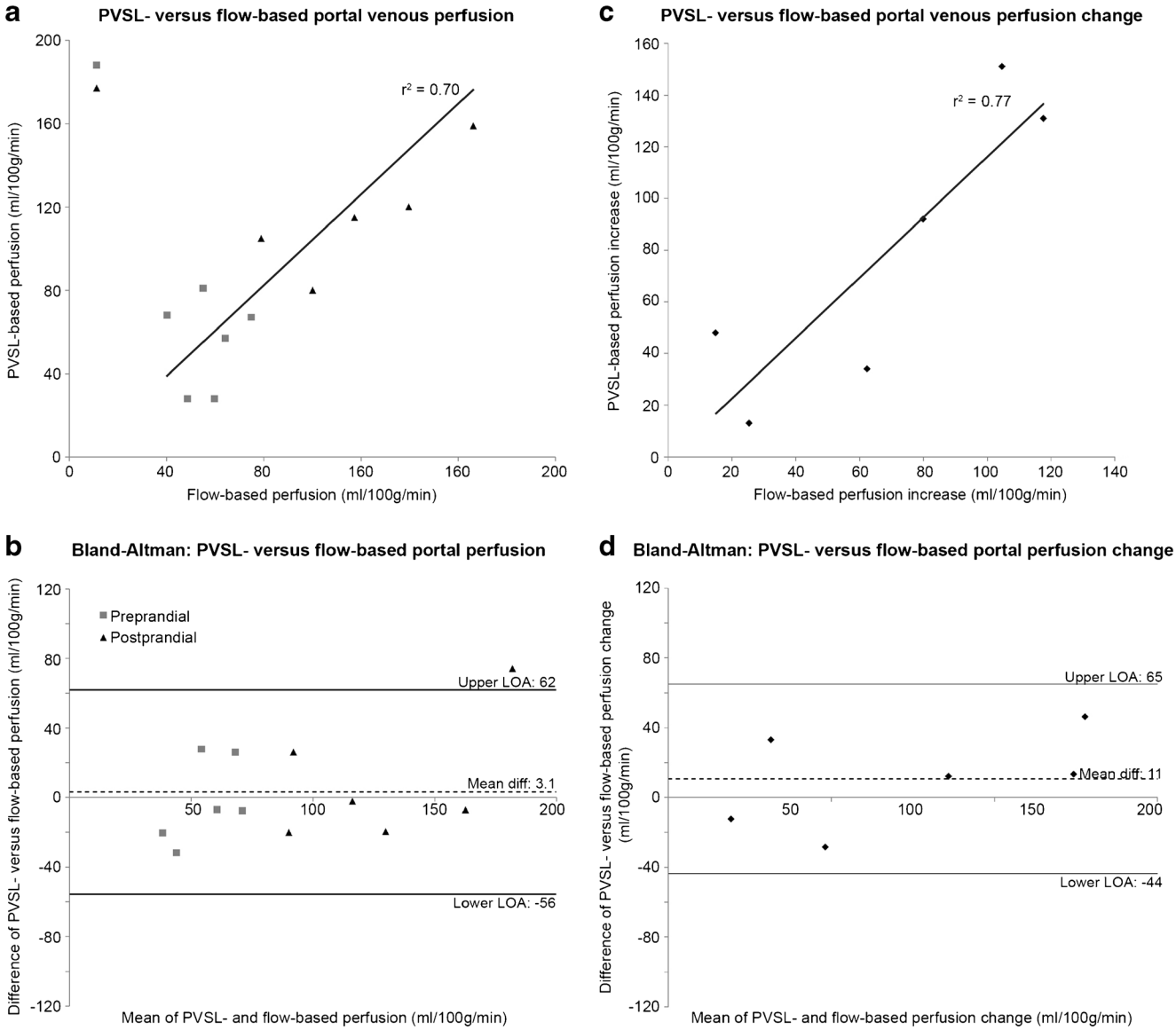

Fig. 5 PVSL-based versus flow-based portal venous perfusion. **a** PVSL-based versus flow-based portal venous liver perfusion (N=6) displaying a correlation of r^2=0.70. **b** Bland-Altman plot of PVSL- versus flow-based portal venous liver perfusion (N=6). Horizontal lines denote the mean difference, and limits-of-agreement (LOA, mean difference ±1.96*SD). **c** PVSL-based versus flow-based portal venous liver perfusion change after meal ingestion (N=6) displaying a correlation of r^2=0.77. **d** Bland-Altman plot of PVSL- versus flow-based portal venous liver perfusion change after meal ingestion (N=6). Horizontal lines denote the mean difference, and limits-of-agreement (LOA, mean difference ±1.96*SD)

We found a significant increase in portal venous perfusion after meal ingestion (63±23 versus 132±42 ml/100g/min, $p<0.05$) in 12 healthy subjects. Its accuracy was tested and confirmed by comparison of the change in liver perfusion with MRI flow measurements of the portal vein in six of the subjects. Perfusion based on both techniques was comparable, demonstrated by small differences between the mean PVSL- and flow-based values for the portal perfusion (mean 3.1 ml/100g/min with 95 % LOA [-56, 62]) as well as the postprandial increase (mean 11 ml/100g/min with 95 % LOA [-44, 65]).

The arterial perfusion obtained with ASL was lower than the portal venous perfusion (35±22 and 22±30 ml/100g/min, pre- and postprandially), as is expected in healthy volunteers. We found a lower mean arterial perfusion postprandially than preprandially, but without a significant difference. The postprandial arterial perfusion decrease could be explained by the hepatic arterial buffer response (HABR), which is a mechanism for controlling hepatic blood flow. If the portal blood flow increases, the arterial hepatic flow decreases and vice versa [22, 23]. A postprandial increase in the portal blood flow is primarily

Table 3 Results

	Preprandial		Postprandial		Perf. Change	t-test
	mean±SD	[min, max]	mean±SD	[min, max]	mean±SD	
Portal venous perfusion (N=12)						
PVSL	63±23	[28, 102]	132±42	[69, 219]	68±48	** p<0.001
Portal venous perfusion (subgroup, N=6)						
PVSL	55±22	[28, 81]	133±49	[80, 219]	78±55	** p=0.018
Based on PV flow	57±12	[40, 75]	124±32	[79, 166]	67±42	** p=0.011
Arterial perfusion (N=12)						
ASL	35±22	[2, 66]	22±30	[-15, 84]	-14±41	p=0.270

All perfusion values are given in [ml/100g/min]. The paired samples Student's t-test has been used to test for significant difference (**, $p<0.05$) between pre- versus postprandial perfusion measures. The flow-based portal perfusion was calculated with PV flow measurements of 14±4.2 ml/s pre- and 30±11 ml/s postprandially. **Abbreviations**: Perf. = Perfusion, SD=standard deviation, Sign.diff. = significant difference, PVSL=portal venous spin labelling, ASL=arterial spin labelling, PV=portal vein, HA=hepatic artery

related to a meal-induced splanchnic vasodilation and subsequent flow increase in the superior mesenteric vein [14].

Comparison to the literature

In the literature, the arterial, portal, and combined perfusion values differed between studies and showed large standard deviations (see Table 4). The selective portal perfusion we found is in range with the literature, although comparison is hindered by the wide range of values in healthy subjects.

Our postprandial portal perfusion is comparable to the studies using other modalities than SL-MRI, e.g. a mean of 102 ml/100ml/min in [24] (CE-CT, unknown prandial status) and a mean of 126.3 ml/100g/min in [25] (CE-MRI, preprandial status). The preprandial portal perfusion we found is lower than the literature values, although the PVSL-based perfusion change correlated well with the flow-based perfusion change ($r^2=0.77$). These portal venous flow values, both pre- and postprandially, are closely comparable to [11, 13, 26], strengthening the comparison of the PVSL-based perfusion with the flow-based perfusion.

Portal blood flow peaks around 30-60 minutes after meal ingestion [27], suggesting we, indeed, scanned around peak flow.

The postprandial arterial perfusion we found is in line with the other studies, especially with [24], concerning 24 control subjects. The preprandial arterial perfusion is slightly higher than that from the studies using CE-MRI and CE-CT.

Comparison of our results to the SL-MRI literature is hindered by the low number of peer-reviewed studies [12] and the concise information in the studies published in proceedings [10, 11, 13].

Gach et al. [10] pioneered selective arterial and portal perfusion in one healthy subject, showing perfusion values in keeping with our results. Katada et al. ([12], N=5) also addressed selective SL imaging, although only of the portal venous supply. The reported mean portal perfusion of 254.3 ml/100g/min was an overestimation compared to portography with CT in the same patients, and is evidently higher than the other reported perfusion values, including our results.

Hoad et al. [11] and Cox et al. [13] addressed solely aselective SL-MRI and calculated combined arterial and portal perfusion, expectedly resulting in higher perfusion values than our selective perfusion values. Hoad et al. [11] found perfusion rates with SL-MRI comparable to dynamic contrast-enhanced (DCE) MRI in 36 chronic liver disease patients and 5 healthy volunteers. Cox et al. [13] presented respectable perfusion images of liver and kidneys. Their liver perfusion values, estimated from the bar plots, were higher in healthy subjects than in compensated cirrhosis patients.

The breathing challenge was tackled by synchronization to a fixed TR of 6500 ms and fitted the breathing cycle comfortably in all subjects without exception. Due to the easy application in healthy subjects and only minor alteration of the natural breathing cycle, we expect no problems with this strategy in patients.

Advantages of SL-MRI for the liver

Selective SL-MRI has interesting advantages for liver imaging. Since it is non-invasive, SL-MRI avoids the risks of nephrogenic systemic fibrosis [28] and is suitable for patients with impaired renal function. Clinical settings, in which the use of contrast agents is contraindicated, could benefit from this technique. Specifically, the perfused and non-perfused regions during and after minimal invasive hepatic tumour ablation techniques such as radiofrequency ablation (RFA) or high-intensity-focused-ultrasound (HIFU), could be assessed repeatedly. Due to

Table 4 Literature values for liver perfusion in healthy volunteers

	Peer-reviewed	Spin-labelling based perfusion			Phase-contrast based flow of the portal vein		Study population
		Arterial and portal	Arterial	Portal	Flow-based perfusion	[ml/s]	
Our results							
Preprandial			35±22	63±22	57±12	14±4	12 healthy subjects, portal flow in 6 subjects
Postprandial			22±30	132±42	125±32	30±11	
Literature: hepatic spin labelling MRI							
Gach et al. [10]	no	148	32	75			1 healthy subject
(ISMRM 2002)							
Hoad et al. [11]	no	114±62				15±5	5 healthy subjects, scanned twice
(ISMRM 2011)		*146±62*					*36 patients with chronic liver disease*
Katada et al. [12]	yes			254.3±58.3 (a)			5 healthy subject
(Jpn J Radiol 2012)							
Cox et al. [13]	no	190±10 (b)				10±2 (b)	30 healthy subjects
(ISMRM 2013)		*140±10 (b)*				*12±4 (b)*	*30 compensated cirrhosis patients*
Literature: other modalities							
Weidekamm et al. [24]	yes	122±39 (c)	20±8 (c)	102±35 (c)			24 control subjects
(AJR 2005, CE-CT)		*102±31 (c)*	*29±21 (c)*	*72±23 (c)*			*41 cirrhotic patients*
Hagiwara et al. [25]	yes	138.4±68.9	6.0±5.1	126.3±66.7			10/27 patients without fibrosis
(Radiology 2008, CE-MRI)		*99.6±39.4*	*10.8±6.8*	*88.7±43.2*			*8/27 patients with fibrosis stage 1-3*
		110.7±68.9	*20.9±19.1*	*89.7±103.7*			*9/27 patients with fibrosis stage 4*
Pazahr et al. [26]	yes					11±3.4	10 healthy subjects, scanned twice preprandial
(Inv Radiol 2013, phase-contrast MRI sequence)						22±4.5	postprandial (after a protein rich meal)
						29±7.0	postprandial (after a carbohydrate-rich meal)

Overview of hepatic perfusion values for our study, articles using hepatic SL-MRI, and articles using other modalities. In italic the perfusion values found for patients in these studies. Values are given as mean±SD. Perfusion values are in [ml/100g/min], unless otherwise indicated. **SL techniques**: The SL studies used pulsed techniques (Hoad et al. and Cox et al.: FAIR, Katada et al.: QUIPPS), except for Gach et al. who used a continuous labelling technique. **ROI**: The ROI was for Hoad et al. a parenchymal mask with exclusion of large vessels, likewise our approach. Katada et al. used parenchymal ROIs of at least 100 mm^2. ROIs were not described by Gach et al. and Cox et al. **Prandial status**: Hoad et al. scanned after an overnight fast, Hagiwara et al. after 6 hours fasting and Pazahr et al. scanned after 8 hours overnight fast for preprandial measurements. For the other articles the prandial status was not described. **Notes**: (a) Values for TI=3000 ms. For 12 patients with hepatocellular carcinoma (HCC) SL-perfusion was compared to CE-CT-based perfusion and showed an overestimation using SL for regions without HCC (mean difference 114.76 ml/min/100g, limits-of-agreement 0.03 - 229.49). Separate SL-perfusion values for the 12 patients were not reported. (b) Values estimated from graph. (c) Values in [ml/100ml/min]. **Abbreviations**: SL=Spin Labelling. CE=contrast-enhanced. CT=computed tomography. ROI=region-of-interest

unknown safety profiles of current Gd-based contrast agents during heating [29], usage is not yet allowed during these interventions.

Furthermore, selective SL-MRI provides direct imaging of the arterial and portal venous blood supply, instead of discrimination on different contrast bolus arrival times. The arterial and portal venous perfusion fraction of focal lesions could potentially be obtained, although further research is needed before SL-MRI could be used to identify an increased arterial blood supply in malignancies [30]. Meanwhile, metastatic renal cell carcinoma has already been successfully imaged using the ASL-MRI technique [6], as well as liver metastases in a mice model [31, 32].

Limitations

This study has several limitations. First, the perfusion quantification is susceptible to uncertainties in the required physical and physiological parameters, such as the bolus arrival time, labelling efficiency, and the T1 of blood (Table 2). Although the parameter values were carefully selected from the literature or experimentally determined, equal parameter values were applied for all volunteers pre- and postprandially. Subject-specific and voxel-wise assessment of bolus arrival times could further improve the quantification accuracy. In future studies, multi-TI sequences [33] would allow estimation of the initial transit time and improve model fitting in general. Furthermore, the quantification model described by Buxton et al. [19] was developed for application to the brain and might not be optimal for portal venous and arterial hepatic perfusion.

Second, negative perfusion rates were found in larger vessels, but not in the liver parenchyma. As we aimed at imaging parenchymal perfusion, large vessels were excluded from the analysis based on a large deviation from the mean signal of the PVSL images.

Third, determination of protocol parameters (TI, TR, labelling duration, and delay) were based on the literature and preliminary experiments (see Fig. 2), but still lack dedicated values for the liver. Since this study aimed at feasibility, we did not perform extensive optimization of the protocol parameters, nor development of respiratory-triggered sequences, nor motion correction during post-processing.

Fourth, this study lacks a gold-standard for the arterial and portal venous perfusion values measured by selective SL-MRI. Therefore, we focused on the individual postprandial perfusion change and compared our results to perfusion values based on MRI flow measurements of the portal vein and values from the literature (Table 4).

Future research

This study proves the feasibility of hepatic SL-MRI, but a thorough investigation of the optimal SL-MRI technique for the liver was beyond the scope of this study. Since only a few studies address hepatic SL-MRI, there is yet limited liver-specific information. However, in this rapidly developing field, further improvements for the application of SL-MRI in the liver are reserved for future investigations.

Future research should include elaborate determination of protocol parameters (TI, TR, pre-saturation, vascular crushing, etc.) and of quantification parameters (slice-specific transit times, measurement of $\Delta M(t)$, T1 value of blood, etc.). Exploration of other labelling strategies is recommended, as e.g. pseudo-continuous labelling techniques might be suitable for portal perfusion examination as well. Standardization of the experiments (meals, fasting hours) and reproducibility measurements will help future analysis. We foresee no problems applying this technique in patients and its non-invasive nature allows for direct application in clinical settings.

Conclusion

In conclusion, this study shows the feasibility of selective spin labelling MRI as a non-invasive technique for the assessment of separate arterial and portal venous liver perfusion. Spin labelling-based portal venous perfusion showed a significant postprandial increase and correlated well with perfusion based on portal venous flow measurements. This non-invasive technique could benefit clinical settings where use of contrast agents is contraindicated.

Acknowledgments We acknowledge MeVis Medical Solutions (Bremen, Germany) for the use of MeVisLab for the quantitative analysis in this study. We would like to thank Jill de Vis for her contributions in performing the experiments.

The scientific guarantor of this publication is M. van Stralen, PhD. The authors of this manuscript declare no relationships with any companies whose products or services may be related to the subject matter of the article. The authors state that this work has not received any funding. No complex statistical methods were necessary for this paper. The Institutional Review Board approved the study. Written informed consent was obtained from all study subjects. Methodology: prospective, experimental study, performed at one institution.

References

1. Pandharipande PV, Krinsky GA, Rusinek H, Lee VS (2005) Perfusion imaging of the liver: current challenges and future goals. Radiology 234(3):661–673
2. Sommer WH, Sourbron S, Huppertz A, Ingrisch M, Reiser MF, Zech CJ (2012) Contrast agents as a biological marker in magnetic resonance imaging of the liver: conventional and new approaches. Abdom Imaging 37(2):164–179
3. Alsop DC, Detre JA, Golay X, Gunther M, Hendrikse J, Hernandez-Garcia L, Lu H, Macintosh BJ, Parkes LM, Smits M, van Osch MJ, Wang DJ, Wong EC, Zaharchuk G (2014) Recommended implementation of arterial spin-labeled perfusion

MRI for clinical applications: A consensus of the ISMRM perfusion study group and the European consortium for ASL in dementia. Magnetic resonance in medicine: official journal of the Society of Magnetic Resonance in Medicine / Society of Magnetic Resonance in Medicine
4. Detre JA, Zhang W, Roberts DA, Silva AC, Williams DS, Grandis DJ, Koretsky AP, Leigh JS (1994) Tissue specific perfusion imaging using arterial spin labeling. NMR Biomed 7(1–2):75–82
5. Edelman RR, Siewert B, Darby DG, Thangaraj V, Nobre AC, Mesulam MM, Warach S (1994) Qualitative mapping of cerebral blood flow and functional localization with echo-planar MR imaging and signal targeting with alternating radio frequency. Radiology 192(2):513–520
6. De Bazelaire C, Rofsky NM, Duhamel G, Michaelson MD, George D, Alsop DC (2005) Arterial spin labeling blood flow magnetic resonance imaging for the characterization of metastatic renal cell carcinoma(1). Acad Radiol 12(3):347–357
7. Notohamiprodjo M, Reiser MF, Sourbron SP (2010) Diffusion and perfusion of the kidney. Eur J Radiol 76(3):337–347
8. Artz NS, Sadowski EA, Wentland AL, Grist TM, Seo S, Djamali A, Fain SB (2011) Arterial spin labeling MRI for assessment of perfusion in native and transplanted kidneys. Magn Reson Imaging 29(1):74–82
9. Wong EC (2007) Vessel-encoded arterial spin-labeling using pseudocontinuous tagging. Magn Reson Med: Off J Soc Magn Reso Med Soc Magn Reson Med 58(6):1086–1091
10. Gach HM, Lopez-Talavera JC, Kam AW (2002) Liver Perfusion MRI using Arterial Spin Labeling. Proceedings of the 10th Annual Meeting of ISMRM, Honolulu
11. Hoad C, Costigan C, Marciani L, Kaye P, Spiller R, Gowland P, Aithal G, Francis S (2011) Quantifyling Blood Flow and Perfusion in Liver Tissue using Phase Contrast Angiography and Arterial Spin Labeling. Proceedings of the 19th Annual Meeting of ISMRM, Montréal
12. Katada Y, Shukuya T, Kawashima M, Nozaki M, Imai H, Natori T, Tamano M (2012) A comparative study between arterial spin labeling and CT perfusion methods on hepatic portal venous flow. Jpn J Radiol 30(10):863–869
13. Cox EF, Ghezzi A, Bennet A, Patel M, Jackson A, Harman D, Costigan C, Farhayu Omar N, James MW, Ryder SD, Gowland PA, Aithal GP, Neil Guha I, Francis ST (2013) A novel MRI protocol to examine haemodynamic compartments in compensated liver cirrhosis. Proceedings of the 21st Annual Meeting of ISMRM, Salt Lake City
14. Tsukuda T, Ito K, Koike S, Sasaki K, Shimizu A, Fujita T, Miyazaki M, Kanazawa H, Jo C, Matsunaga N (2005) Pre- and postprandial alterations of portal venous flow: evaluation with single breath-hold three-dimensional half-Fourier fast spin-echo MR imaging and a selective inversion recovery tagging pulse. J Magn Reson Imaging: JMRI 22(4):527–533
15. Patel MR, Siewert B, Warach S, Edelman RR (1995) Diffusion and perfusion imaging techniques. Magn Reson Imaging Clin N Am 3(3): 425–438
16. Wu WC, Fernandez-Seara M, Detre JA, Wehrli FW, Wang J (2007) A theoretical and experimental investigation of the tagging efficiency of pseudocontinuous arterial spin labeling. Magn Reson Med: Off J Soc Magn Reson Med Soc Magn Reson Med 58(5):1020–1027
17. Wong EC (2005) Quantifying CBF, with pulsed ASL: technical and pulse sequence factors. J Magn Reson Imaging: JMRI 22(6):727–731
18. Silva AC, Kim SG (1999) Pseudo-continuous arterial spin labeling technique for measuring CBF dynamics with high temporal resolution. Magn Reson Med: Off J Soc Magn Reson Med Soc Magn Reson Med 42(3):425–429
19. Buxton RB, Frank LR, Wong EC, Siewert B, Warach S, Edelman RR (1998) A general kinetic model for quantitative perfusion imaging with arterial spin labeling. Magn Reson Med: Off J Soc Magn Reson Med Soc Magn Reson Med 40(3):383–396
20. Wang X, Xue HD, Jin ZY, Su BY, Li Z, Sun H, Chen Y, Liu W (2013) Quantitative hepatic CT perfusion measurement: comparison of Couinaud's hepatic segments with dual-source 128-slice CT. Eur J Radiol 82(2):220–226
21. Petersen ET, Zimine I, Ho YC, Golay X (2006) Non-invasive measurement of perfusion: a critical review of arterial spin labelling techniques. Br J Radiol 79(944):688–701
22. Eipel C, Abshagen K, Vollmar B (2010) Regulation of hepatic blood flow: the hepatic arterial buffer response revisited. World J Gastroenterol: WJG 16(48):6046–6057
23. Lafortune M, Dauzat M, Pomier-Layrargues G, Gianfelice D, Lepanto L, Breton G, Marleau D, Dagenais M, Lapointe R (1993) Hepatic artery: effect of a meal in healthy persons and transplant recipients. Radiology 187(2):391–394
24. Weidekamm C, Cejna M, Kramer L, Peck-Radosavljevic M, Bader TR (2005) Effects of TIPS on liver perfusion measured by dynamic CT. AJR Am J Roentgenol 184(2):505–510
25. Hagiwara M, Rusinek H, Lee VS, Losada M, Bannan MA, Krinsky GA, Taouli B (2008) Advanced liver fibrosis: diagnosis with 3D whole-liver perfusion MR imaging–initial experience. Radiology 246(3):926–934
26. Pazahr S, Nanz D, Rossi C, Chuck N, Stenger I, Wurnig MC, Schick F, Boss A (2014) Magnetic resonance imaging of the liver: apparent diffusion coefficients from multiexponential analysis of b values greater than 50 s/mm2 do not respond to caloric intake despite increased portal-venous blood flow. Investig Radiol 49(3):138–146
27. Iwao T, Toyonaga A, Shigemori H, Oho K, Sakai T, Tayama C, Masumoto H, Sato M, Tanikawa K (1996) Hepatic artery hemodynamic responsiveness to altered portal blood flow in normal and cirrhotic livers. Radiology 200(3):793–798
28. Endre ZH (2007) Nephrogenic systemic fibrosis: is any contrast safe in renal failure? Int Med J 37(7):429–431
29. Hijnen NM, Elevelt A, Grull H (2013) Stability and trapping of magnetic resonance imaging contrast agents during high-intensity focused ultrasound ablation therapy. Investig Radiol 48(7):517–524
30. Wang LM, Jani AR, Hill EJ, Sharma RA (2013) Anatomical basis and histopathological changes resulting from selective internal radiotherapy for liver metastases. J Clin Pathol 66(3):205–211
31. Johnson SP, Ramasawmy R, Campbell-Washburn A, Robson M, Wells J, Rajkumar V, Walker-Samuel S, Lythgoe MF, Pedley RB (2013) Comparison of Arterial Spin Labelling and R2* as Predictive Response Biomarkers for Vascular Targeting Agents in Liver Metastases. Proceedings of the 21st Annual Meeting of ISMRM, Salt Lake City
32. Ramasawmy R, Walker-Samuel S, Campbell A, Johnson SP, Wells J, Pedley RB, Lythgoe MF (2012) Look-Locker Arterial Spin Labelling (ASL) of Liver Metastases. Proceedings of the 20th Annual Meeting of ISMRM, Melbourne
33. Gunther M, Bock M, Schad LR (2001) Arterial spin labeling in combination with a look-locker sampling strategy: inflow turbo-sampling EPI-FAIR (ITS-FAIR). Magn Reson Med: Off J Soc Magn Reson Med Soc Magn Reson Med 46(5):974–984
34. Sharma P, Socolow J, Patel S, Pettigrew RI, Oshinski JN (2006) Effect of Gd-DTPA-BMA on blood and myocardial T1 at 1.5 T and 3 T in humans. J Magn Reson Imaging: JMRI 23(3):323–330
35. de Bazelaire CM, Duhamel GD, Rofsky NM, Alsop DC (2004) MR imaging relaxation times of abdominal and pelvic tissues measured in vivo at 3.0 T: preliminary results. Radiology 230(3): 652–659
36. Kosturski NMS, Vutov Y (2011) Comparison of Two Techniques for Radiofrequency Hepatic Tumor Ablation through Numerical Simulation. AIP Conf Proc 1404:431